J|A|C|S
ARTICLES
Published on Web 10/09/2004

Length-Dependent Transport in Molecular Junctions Based on SAMs of Alkanethiols and Alkanedithiols: Effect of Metal Work Function and Applied Bias on Tunneling Efficiency and Contact Resistance

Vincent B. Engelkes,[†] Jeremy M. Beebe,[‡] and C. Daniel Frisbie*,[†]

Contribution from the Department of Chemical Engineering and Materials Science and Department of Chemistry, University of Minnesota, Minneapolis, Minnesota 55455

Received June 23, 2004; E-mail: frisbie@cems.umn.edu

Abstract: Nanoscopic tunnel junctions were formed by contacting Au-, Pt-, or Ag-coated atomic force microscopy (AFM) tips to self-assembled monolayers (SAMs) of alkanethiol or alkanedithiol molecules on polycrystalline Au, Pt, or Ag substrates. Current−voltage traces exhibited sigmoidal behavior and an exponential attenuation with molecular length, characteristic of nonresonant tunneling. The length-dependent decay parameter, β, was found to be approximately 1.1 per carbon atom (C^{-1}) or 0.88 $Å^{-1}$ and was independent of applied bias (over a voltage range of ±1.5 V) and electrode work function. In contrast, the contact resistance, R_0, extrapolated from resistance versus molecular length plots showed a notable decrease with both applied bias and increasing electrode work function. The doubly bound alkanedithiol junctions were observed to have a contact resistance approximately 1 to 2 orders of magnitude lower than the singly bound alkanethiol junctions. However, both alkanethiol and dithiol junctions exhibited the same length dependence (β value). The resistance versus length data were also used to calculate transmission values for each type of contact (e.g., Au−S−C, Au/CH_3, etc.) and the transmission per C−C bond (T_{C-C}).

Introduction

A variety of methods are currently available for probing the electrical conductance of discrete molecules or clusters of molecules sandwiched between metal or semiconductor electrodes. These methods include incorporating test molecules into metal-capped nanopores,[1−3] placing them in gaps between crossed wires[4,5] or wires with nanoscopic breaks (cracks),[6,7] or contacting molecular monolayers with conducting mercury drops[8−11] or scanning probe microscopy tips.[12−18] The overall aim of fundamental molecular conductance studies is to establish how the structure and electronic properties of molecules and their associated contacts affect the current−voltage ($I-V$) characteristics observed for the junction. Transport phenomena reported for molecular junctions include negative differential resistance,[1,19,20] rectification,[10,11,21] conductance quantization,[22,23] and switching.[24−26]

The importance of metal−molecule or semiconductor−molecule interfaces in determining junction $I-V$ characteristics

[†] Department of Chemical Engineering and Materials Science.
[‡] Department of Chemistry.

(1) Chen, J.; Reed, M. A.; Rawlett, A. M.; Tour, J. M. *Science* **1999**, *286*, 1550−1552.
(2) Chen, J.; Calvet, L. C.; Reed, M. A.; Carr, D. W.; Grubisha, D. S.; Bennett, D. W. *Chem. Phys. Lett.* **1999**, *313*, 741−748.
(3) Wang, W.; Lee, T.; Reed, M. A. *Phys. Rev. B* **2003**, *68*, 035416/035411−035416/035417.
(4) Kushmerick, J. G.; Holt, D. B.; Pollack, S. K.; Ratner, M. A.; Yang, J. C.; Schull, T. L.; Naciri, J.; Moore, M. H.; Shashidhar, R. *J. Am. Chem. Soc.* **2002**, *124*, 10654−10655.
(5) Kushmerick, J. G.; Holt, D. B.; Yang, J. C.; Naciri, J.; Moore, M. H.; Shashidhar, R. *Phys. Rev. Lett.* **2002**, *89*, 086802/086801−086802/086804.
(6) Reed, M. A.; Zhou, C.; Muller, C. J.; Burgin, T. P.; Tour, J. M. *Science* **1997**, *278*, 252−254.
(7) Park, H.; Park, J.; Lim, A. K. L.; Anderson, E. H.; Alivisatos, A. P.; McEuen, P. L. *Nature* **2000**, *407*, 58−60.
(8) Slowinski, K.; Chamberlain, R. V., II; Bilewicz, R.; Majda, M. *J. Am. Chem. Soc.* **1996**, *118*, 4709−4710.
(9) Holmlin, R. E.; Haag, R.; Chabinyc, M. L.; Ismagilov, R. F.; Cohen, A. E.; Terfort, A.; Rampi, M. A.; Whitesides, G. M. *J. Am. Chem. Soc.* **2001**, *123*, 5075−5085.
(10) Selzer, Y.; Salomon, A.; Cahen, D. *J. Phys. Chem. B* **2002**, *106*, 10432−10439.
(11) Liu, Y.-J.; Yu, H.-Z. *ChemPhysChem* **2003**, *4*, 335−342.
(12) Wold, D. J.; Frisbie, C. D. *J. Am. Chem. Soc.* **2000**, *122*, 2970−2971.
(13) Wold, D. J.; Frisbie, C. D. *J. Am. Chem. Soc.* **2001**, *123*, 5549−5556.
(14) Wold, D. J.; Haag, R.; Rampi, M. A.; Frisbie, C. D. *J. Phys. Chem. B* **2002**, *106*, 2813−2816.
(15) Cui, X. D.; Zarate, X.; Tomfohr, J.; Sankey, O. F.; Primak, A.; Moore, A. L.; Moore, T. A.; Gust, D.; Harris, G.; Lindsay, S. M. *Nanotechnology* **2002**, *13*, 5−14.
(16) Labonte, A. P.; Tripp, S. L.; Reifenberger, R.; Wei, A. *J. Phys. Chem. B* **2002**, *106*, 8721−8725.
(17) Fan, F.-R. F.; Yao, Y.; Cai, L.; Cheng, L.; Tour, J. M.; Bard, A. J. *J. Am. Chem. Soc.* **2004**, *126*, 4035−4042.
(18) Liu, B.; Bard, A. J.; Mirkin, M. V.; Creager, S. E. *J. Am. Chem. Soc.* **2004**, *126*, 1485−1492.
(19) Fan, F.-R. F.; Yang, J.; Cai, L.; Price, D. W., Jr.; Dirk, S. M.; Kosynkin, D. V.; Yao, Y.; Rawlett, A. M.; Tour, J. M.; Bard, A. J. *J. Am. Chem. Soc.* **2002**, *124*, 5550−5560.
(20) Guisinger, N. P.; Greene, M. E.; Basu, R.; Baluch, A. S.; Hersam, M. C. *Nano Lett.* **2004**, *4*, 55−59.
(21) Metzger, R. M. *Chem. Rev.* **2003**, *103*, 3803−3834.
(22) Cui, X. D.; Primak, A.; Zarate, X.; Tomfohr, J.; Sankey, O. F.; Moore, A. L.; Moore, T. A.; Gust, D.; Nagahara, L. A.; Lindsay, S. M. *J. Phys. Chem. B* **2002**, *106*, 8609−8614.
(23) Xiao, X.; Xu, B.; Tao, N. J. *Nano Lett.* **2004**, *4*, 267−271.
(24) Donhauser, Z. J.; Mantooth, B. A.; Kelly, K. F.; Bumm, L. A.; Monnell, J. D.; Stapleton, J. J.; Price, D. W., Jr.; Rawlett, A. M.; Allara, D. L.; Tour, J. M.; Weiss, P. S. *Science* **2001**, *292*, 2303−2307.
(25) Ramachandran, G. K.; Hopson, T. J.; Rawlett, A. M.; Nagahara, L. A.; Primak, A.; Lindsay, S. M. *Science* **2003**, *300*, 1413−1416.
(26) Lau, C. N.; Stewart, D. R.; Williams, R. S.; Bockrath, M. *Nano Lett.* **2004**, *4*, 569−572.

is well recognized,[27−29] yet there have been few direct measures of contact effects in molecular junctions. Recently, Weiss and co-workers have reported scanning tunneling microscopy (STM) evidence that switching behavior of certain conjugated molecules can be related to the molecular tilt angle with respect to the metal substrate. In these systems, the molecules are anchored to a gold surface via a Au−S bond. These workers hypothesize that the orbitals on the terminal S atom must rehybridize when the molecular tilt changes substantially, giving rise to a change in overall conductance of the molecule.[24,30] Others have reported that junction conductance depends dramatically on the strength of metal-molecule bonds. For example, Lindsay and co-workers first reported that the conductance of junctions strongly depended on whether the molecules were chemisorbed or physisorbed to the contacts. Junctions with two "chemicontacts" were orders of magnitude less resistive than junctions with only one chemisorbed contact.[31]

This report describes direct measurements of contact resistance in molecular junctions based on *n*-alkanethiol and *n*-alkanedithiol molecules self-assembled on Au, Ag, and Pt electrodes. It substantially expands our earlier study[32] of metal−(*n*-alkanethiol)−metal junctions in which we demonstrated that the tunneling efficiency parameter (β) and the contact resistance (R_0) could be extracted reproducibly from plots of (low bias) junction resistance versus molecular length. Specifically, we include more electrode combinations, we examine the difference in resistance between *n*-alkanethiols and *n*-alkanedithiols, and we measure the voltage dependence of β and R_0. Questions we address are as follows: (1) what effect do chemisorbed versus physisorbed contacts have on the resistance of molecular junctions, (2) how is the contact resistance affected by the type of metal used for contact, (3) how do the contacts, in terms of both metal work function and type of contact (i.e. chemisorbed versus physisorbed), affect the length dependence of these measurements, and (4) how does the applied bias affect the length dependence and contact resistance of these junctions. Finally, we use the resistance data, combined with an estimate for the number of molecules (N) present in our junctions, to calculate electronic transmission values for specific chemisorbed (e.g., Au−S−C) and physisorbed (e.g., Au/CH_3) contacts.

Figure 1 shows a representation of our conducting probe atomic force microscopy (CP-AFM) approach to junction formation in which we use a metal-coated AFM tip to contact a self-assembled monolayer (SAM) on a metal substrate. Contact to the monolayer is controlled by feedback electronics that are capable of maintaining a set-point load with sub-nN precision. Current−voltage ($I-V$) characteristics are acquired by sweeping the voltage applied to the tip. The advantages of this technique include the ease of junction formation, the ability to change contact metals, and the ability to vary the compressive load on the junction. For this study, it is important to note that because the tip and substrate can be coated with a variety of metals, it is possible to alter the position of the Fermi level with respect to the HOMO and LUMO levels of the molecules. The main requirement for a successful measurement is that the test molecules must form a reasonably ordered monolayer.

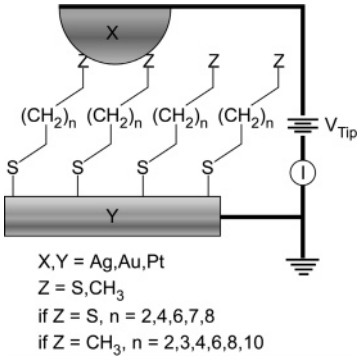

Figure 1. Schematic representation of a molecular tunnel junction formed using CP-AFM. A metal-coated (Au, Ag, or Pt) AFM tip is brought into contact with a SAM of alkanethiols or alkanedithiols of various lengths on a Au-, Ag-, or Pt-coated Si substrate. Voltage is swept at the tip, and the resulting current is measured.

There is a significant body of data in the literature involving electron transport in alkanethiol and alkanedithiol molecules, especially in terms of $I-V$ behavior and length dependence. For the most part, there is good agreement among published reports involving β at low bias, the overall magnitude of measured current, and the shape of the $I-V$ profile. Values for β, at low bias primarily, have been reported[3,13,15,33,34] to be ~0.9 $Å^{-1}$ with the exception of experiments involving degenerately doped p-Si electrodes ($\beta = 0.6$ $Å^{-1}$)[35,36] and single molecule Au−alkanedithiol−Au nanoparticle junctions ($\beta = 0.57$ $Å^{-1}$).[22] β values near 1 $Å^{-1}$ have also been observed in electrochemical experiments involving saturated molecules.[37,38] Currents are generally observed to be sigmoidal functions of voltage (linear at low bias and exponential at higher biases) with low-bias currents ranging between ~0.1 and 0.6 pA for a dodecanethiol molecule at 0.2 V.[3,10,13,32,36,39] Less concrete data exist for the voltage and electrode work function dependence of β and R_0. For example, β has been shown to both increase[10,15] and decrease[22] with applied bias.

Experimental Section

Materials. Gold nuggets (99.999% pure) were purchased from Mowrey, Inc. (St. Paul, MN). Evaporation boats and chromium evaporation rods were purchased from R. D. Mathis (Long Beach, CA). Platinum and titanium for e-beam evaporation were purchased from Kamis, Inc. (Mahopac Falls, NY). Silicon (100) wafers were purchased from WaferNet (San Jose, CA). AFM tips were purchased from Digital Instruments. Ethanol (reagent alcohol) was purchased from Fisher Scientific. All *n*-alkanethiol molecules, 1,4-butanedithiol, and 1,6-hexanedithiol were purchased from Aldrich, and 1,8-octanedithiol, 1,9-nonanedithiol, and 1,10-decanedithiol were purchased from Lancaster Synthesis.

(27) Yaliraki, S. N.; Ratner, M. A. *J. Chem. Phys.* **1998**, *109*, 5036−5043.
(28) Hong, S.; Reifenberger, R.; Tian, W.; Datta, S.; Henderson, J.; Kubiak, C. P. *Superlattices Microstruct.* **2000**, *28*, 289−303.
(29) Seminario, J. M.; De La Cruz, C. E.; Derosa, P. A. *J. Am. Chem. Soc.* **2001**, *123*, 5616−5617.
(30) Donhauser, Z. J.; Mantooth, B. A.; Pearl, T. P.; Kelly, K. F.; Nanayakkara, S. U.; Weiss, P. S. *Jpn. J. Appl. Phys.* **2002**, *41*, 4871−4877.
(31) Cui, X. D.; Primak, A.; Zarate, X.; Tomfohr, J.; Sankey, O. F.; Moore, A. L.; Moore, T. A.; Gust, D.; Harris, G.; Lindsay, S. M. *Science* **2001**, *294*, 571−574.
(32) Beebe, J. M.; Engelkes, V. B.; Miller, L. L.; Frisbie, C. D. *J. Am. Chem. Soc.* **2002**, *124*, 11268−11269.
(33) Slowinski, K.; Fong, H. K. Y.; Majda, M. *J. Am. Chem. Soc.* **1999**, *121*, 7257−7261.
(34) Holmlin, R. E.; Ismagilov, R. F.; Haag, R.; Mujica, V.; Ratner, M. A.; Rampi, M. A.; Whitesides, G. M. *Angew. Chem., Int. Ed.* **2001**, *40*, 2316−2320.
(35) Selzer, Y.; Salomon, A.; Cahen, D. *J. Am. Chem. Soc.* **2002**, *124*, 2886−2887.
(36) Liu, Y.-J.; Yu, H.-Z. *ChemPhysChem* **2002**, *3*, 799−802.
(37) Smalley, J. F.; Feldberg, S. W.; Chidsey, C. E. D.; Linford, M. R.; Newton, M. D.; Liu, Y.-P. *J. Phys. Chem.* **1995**, *99*, 13141−13149.
(38) Slowinski, K.; Chamberlain, R. V.; Miller, C. J.; Majda, M. *J. Am. Chem. Soc.* **1997**, *119*, 11910−11919.

Sample and Tip Preparation. Silicon substrates and contact mode AFM tips were metal-coated with Au or Ag in a Balzers thermal evaporator at a base pressure of $\sim 2 \times 10^{-6}$ Torr. Films were deposited to a thickness of 1000 Å at a rate of 1 Å/s atop a 50 Å Cr adhesion layer. Pt films (200 Å thick) were deposited with an e-beam evaporator with a 50 Å Ti adhesion layer. SAMs were formed from ~0.5 mM solutions of molecules in ethanol. Substrates were allowed to incubate in solution for at least a few hours to ensure formation of dense monolayers.

Monolayer Characterization. Monolayers were characterized by water (18 MΩ) contact angle, spectroscopic ellipsometry, AFM adhesion forces, and $I-V$ behavior. Contact angles were measured using a telescope and goniometer mounted to a home-built stage. A small drop of water was placed on a sample by a syringe, and the contact angles were observed on both sides of the drop. The values from approximately eight drops were averaged to provide an average contact angle.

Ellipsometry was performed using a Sopra ES4G spectroscopic ellipsometer equipped with a xenon light source. Measurements of the polarization angles Ψ and Δ were taken as a function of wavelength (λ) between 250 and 900 nm at an incident angle of 75°. The indices of refraction ($n(\lambda)$) and extinction coefficients ($k(\lambda)$) of the metal-coated substrates were determined by measurement of the polarization angles prior to monolayer deposition. The instrument software converted these values to $n(\lambda)$ and $k(\lambda)$ by assuming that the substrate was of infinite thickness. After monolayer deposition, the polarization angles were again measured and film thicknesses determined by the instrument software. A parallel layer model was used (substrate/film/ambient) with n and k values of the SAM assumed to be 1.5 and 0, respectively.

Adhesive forces and $I-V$ behavior were examined using a Digital Instruments MultiMode AFM. Pull-off forces were measured in "force calibration mode" from the retraction trace of the cantilever deflection signal as a metal-coated tip was brought into and out of contact once with a SAM-coated substrate. $I-V$ measurements are detailed below.

***I*−*V* Measurements.** Junctions were completed by mounting the substrates in the AFM and bringing the metal-coated tip into contact with the SAM under ~2 nN of applied compressive load (about 10 nN of adhesive force was also present for alkanethiol monolayers, 15 nN for alkanedithiol monolayers). Voltages were applied to the tip with a Keithley model 236 electrometer operated in "DC mode" for "low voltage" experiments (±0.3 V). The resulting junction current was measured at the tip with the 236 and also with a Keithley model 6517 or 617 electrometer connected between the substrate electrode and ground. Operation of the 236 in "DC mode" was controlled with LabVIEW software, which stepped the voltage incrementally allowing for a current resolution of ~1 pA. Speed is sacrificed in this mode, and data cannot be collected faster than about 2 points per second. "High voltage" measurements (±1.5 V) were taken with the 236 electrometer operated in "sweep mode". Here, the 236 was set to store a swept $I-V$ trace in its buffer and later return it to the LabVIEW routine. Acquisitions of this type allowed us to gather 600 data points in ~3 s. Current resolution at this speed was however limited to ~0.2 nA.

For the low voltage experiments (±0.3 V), each metal−molecule−metal combination was examined with about 10 different tips. For a given tip, approximately 5 to 10 $I-V$ traces were collected on 3 to 5 different chain lengths of either alkanethiol or alkanedithiol (i.e., 5−10 traces were acquired on each sample of a given chain length. Examining 3 different chain lengths meant 15−30 separate $I-V$ sweeps with 1 tip). Linear fits to each $I-V$ trace yielded low-bias resistance values that were then averaged for each chain length. Extrapolation of this low-bias average *resistance* versus molecular chain length resulted in a contact resistance, R_0, and a β value for each tip. For a given metal−molecule−metal combination, the corresponding set of R_0 and β values were averaged (R_0 values were geometrically averaged, and outliers were omitted for both parameters according to the Chauvenet criterion) providing a mean and standard deviation of each parameter for all 18 metal−molecule−metal combinations. Importantly, examination of the tips by SEM and by imaging ultra-sharp Silicon calibration samples (TGT01 from MikroMasch) suggested that they had very similar radii and that the number of molecules in each junction was roughly the same. We will return to the number of molecules in the junction in the Discussion section.

High voltage behavior (±1.5 V) was characterized only on Au−alkanethiol−Au and Au−alkanedithiol−Au junctions. For each molecule, approximately 25 $I-V$ traces were collected for 3 or 4 different chain lengths and then geometrically averaged for each length. To determine the voltage dependence of R_0 and β, an extrapolation of the logarithm of mean *current* versus chain length was performed at each voltage on a point-by-point basis along the collected voltage window. This resulted in a value for β and R_0 at each applied voltage.

Results

Monolayer Characterization. Alkanethiol monolayers exhibited large water contact angles, increasing with chain length to about 110° for dodecanethiol. The increase in contact angle is indicative of improving film order with increase in chain length. Alkanedithiol monolayers exhibited notably lower wetting angles ranging between 55° for butanedithiol and 70° for decanedithiol, indicating the presence of a terminal thiol group. Plots of alkanethiol ellipsometric thickness versus the number of carbon atoms in the chain (between 4 and 16) were observed to have slopes of 1.29, 1.20, and 1.28 Å per carbon atom (±0.05) for Ag, Au, and Pt substrates, respectively. These slopes indicate that the films are very well-formed.[40,41] Thickness measurements on alkanedithiol monolayers were comparable to the analogous alkanethiol monolayers, indicating that the molecules are not hairpinned to the surface and are standing upright. However, there was a larger spread in thickness values and fewer chain lengths available (compared to the monothiols) to provide accurate slopes of thickness versus chain length.

Further evidence that the alkanedithiol monolayers are upright was provided by measured adhesive forces between metal-coated AFM tips and the monolayers. Adhesions were observed to be larger on alkanedithiol monolayers than on alkanethiol monolayers (~15 nN compared to ~10 nN). Electrical characterization also provided indication that the alkanedithiol monolayers were not hairpinned to the surface. The measured β values for the alkanethiol and alkanedithiol monolayers were the same, indicating the same scaling of the film thickness with chain length. Current asymmetry, which is not highlighted in this paper, also indicates that the contacts on either end of the alkanedithiol monolayers are similar. In the case of alkanethiol monolayers, slightly more current is consistently observed when the tip is biased negatively relative to the substrate. This asymmetry completely vanishes with alkanedithiol monolayers. Other groups have also published X-ray photoemission spec-

(39) Salomon, A.; Cahen, D.; Lindsay, S.; Tomfohr, J.; Engelkes, V. B.; Frisbie, C. D. *Adv. Mater.* **2003**, *15*, 1881−1890.
(40) Porter, M. D.; Bright, T. B.; Allara, D. L.; Chidsey, C. E. D. *J. Am. Chem. Soc.* **1987**, *109*, 3559−3568.
(41) Bain, C. D.; Troughton, E. B.; Tao, Y. T.; Evall, J.; Whitesides, G. M.; Nuzzo, R. G. *J. Am. Chem. Soc.* **1989**, *111*, 321−335.

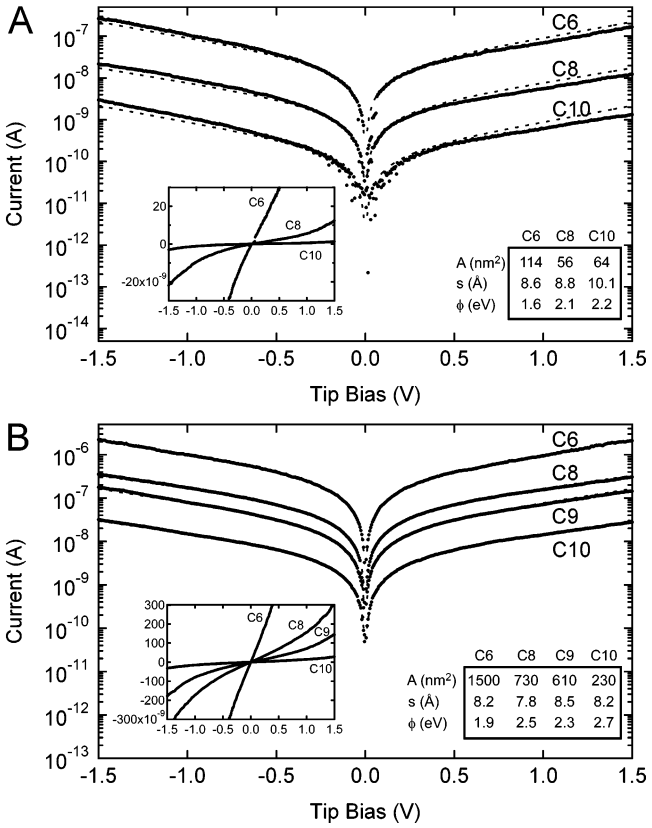

Figure 2. Representative semilog plot of $I-V$ traces of C6, C8, and C10 Au−alkanethiol−Au (A) and Au−alkanedithiol−Au (B) junctions (absolute value of current is displayed). Dashed lines are fits to eq 1, and fit parameters are displayed in table form. Insets show sigmoidal $I-V$ behavior on linear axes.

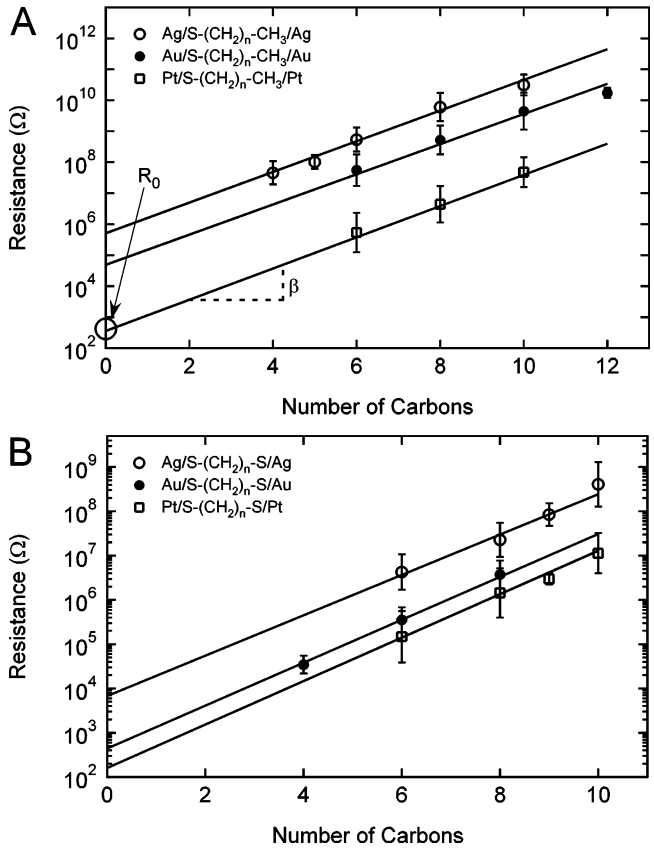

Figure 3. Resistance versus length plots for alkanethiol (A) and alkanedithiol (B) junctions. Data points are average resistance values of about 10 experiments performed with different tips. Lines are not least-squares fits to the data but are defined by the average R_0 and β values for the same set of tips.

troscopy (XPS) data on alkanedithiol monolayers that show unbound thiol groups.[42−44]

General $I-V$ Behavior. Figure 2 shows that current−voltage traces of representative Au−S−$(CH_2)_n$−CH_3/Au and Au−S−$(CH_2)_n$−S−Au junctions behave sigmoidally according to the Simmons equation for tunneling through a square barrier:[45]

$$I = \frac{qA}{4\pi^2\hbar s^2}\left\{\left(\phi - \frac{qV}{2}\right)\cdot\exp\left(-\frac{2s\sqrt{2m}}{\hbar}\sqrt{\phi - \frac{qV}{2}}\right) - \left(\phi + \frac{qV}{2}\right)\cdot\exp\left(-\frac{2s\sqrt{2m}}{\hbar}\sqrt{\phi + \frac{qV}{2}}\right)\right\} \quad (1)$$

where A is the junction area, s is the width of the barrier, m is the electron mass, and ϕ is the barrier height. In the low-bias regime, current is essentially linear with applied voltage and increases exponentially at higher applied voltages approaching $\phi/2$. Figure 2 also shows an exponential decrease in current with increasing barrier width (length of the molecule). It is believed that the mechanism for transport in these junctions is nonresonant tunneling because (1) it has been observed by others that the temperature dependence of the conductance is weak,[3] (2) the $I-V$ characteristics follow this general form, and (3) at a given voltage, current scales exponentially with length.

At low bias, eq 1 can be used to determine the resistance (R) of the linear regime as follows:

$$R = \frac{4\pi^2\hbar^2 s}{q^2 A\sqrt{2m\phi}}\exp\left(\frac{2\sqrt{2m\phi}s}{\hbar}\right) \quad (2)$$

Although this equation is not strictly exponential in s, it can be approximated as such considering that the exponential factor dominates (i.e., the length dependence of the current in Figure 2 is exponential, not linear). Despite the fact that the Simmons model has inherent flaws for molecular junction systems (see below), the general exponential behavior of eq 2 is observed. Therefore, it is common to replace eq 2 with a simpler formula:

$$R = R_0\exp(\beta n) \quad (3)$$

where R_0 is the effective contact resistance, n is the number of repeat units (in this case carbon atoms), and β is the structure-dependent attenuation factor:

$$\beta = 2\sqrt{\frac{2m\phi}{\hbar^2}} \quad (4)$$

According to eq 3, measured low-bias resistances are plotted versus the number of carbon atoms in the molecular chain on a semilog axis. The fit parameters R_0 and β are extracted experimentally as illustrated in Figure 3; β is the slope of the best-fit line to the data points and R_0 is the y-intercept.

(42) Rieley, H.; Kendall, G. K.; Zemicael, F. W.; Smith, T. L.; Yang, S. *Langmuir* **1998**, *14*, 5147−5153.
(43) Deng, W.; Yang, L.; Fujita, D.; Nejoh, H.; Bai, C. *Appl. Phys. A* **2000**, *71*, 639−642.
(44) Pethkar, S.; Aslam, M.; Mulla, I. S.; Ganeshan, P.; Vijayamohanan, K. *J. Mater. Chem.* **2001**, *11*, 1710−1714.
(45) Simmons, J. G. *J. Appl. Phys.* **1963**, *34*, 1793−1803.

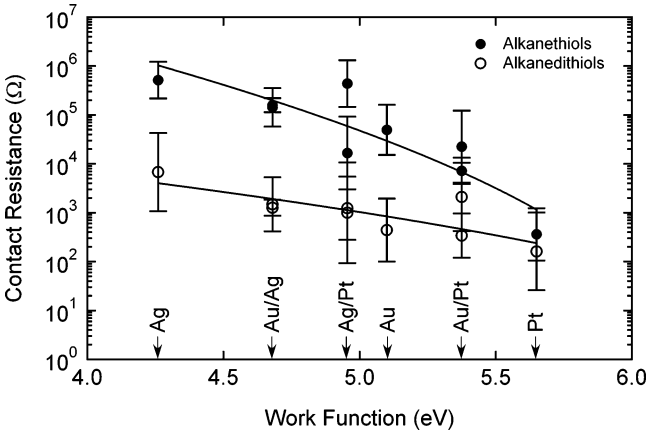

Figure 4. Contact resistance (R_0) as a function of electrode metal work function for junctions composed of alkanethiols (●) and alkanedithiols (○). The solid lines are guides for the eye.

Work Function and Bias Dependence of the Junction Contact Resistance (R_0). Figure 3 shows semilog plots of low-bias resistance versus length for alkanethiol and alkanedithiol SAMs contacted by Ag, Au, or Pt electrodes. The zero length intercepts of these plots represent the contact resistances. For both alkanethiol and alkanedithiol junctions, resistances (at any given chain length) are larger when lower work function metals are used as electrodes. Junction resistances are largest for Ag contacts and smallest for Pt. Au contacts result in resistances that are between that of Ag and Pt junctions. The differences in the junction resistances can be attributed to the differences in the zero length intercepts, i.e., the contact resistance for the individual junctions.

Figure 4 shows a plot of R_0 versus electrode metal work function similar to that published in our initial report,[32] but now including new data from alkanedithiol junctions and more mixed-metal alkanethiol junctions. This plot was generated from the intercepts of Figure 3 along with R_0 points determined for junctions composed of mixed-metal electrodes (e.g., Au/Pt, Ag/Au, etc.). For these mixed metal junctions, we assigned a work function equal to the average of the two metal work functions. This was done because it is observed that the resistances of mixed metal junctions generally fall somewhere between the resistances of the two single metal junctions.

A few observations can be made about Figure 4: (1) the contact resistance decreases with increasing metal work function, (2) junctions composed of two different metal electrodes behave as though the work function is located between that of the two metal work functions involved, (3) junctions with two chemisorbed contacts (alkanedithiols) have a lower contact resistance than those where one contact is physisorbed (alkanethiols), and (4) in doubly bound alkanedithiol junctions, it appears that "reverse cases" of mixed metal junctions (i.e., Au tip/Ag substrate versus Ag tip/Au substrate) are not distinguishable.

We have also investigated the bias dependence of R_0 (Figure 5). As can be seen from the figure, R_0 decreases with increasing bias and the effect is comparable in magnitude to varying the work function. As stated in the Experimental Section, R_0 values at each voltage were determined by extrapolation of the logarithm of current as a function of molecular length. Near zero bias where measured currents are near zero, the logarithm values approach negative infinity. This results in high error of the fit parameters as observed in the scatter of data points near

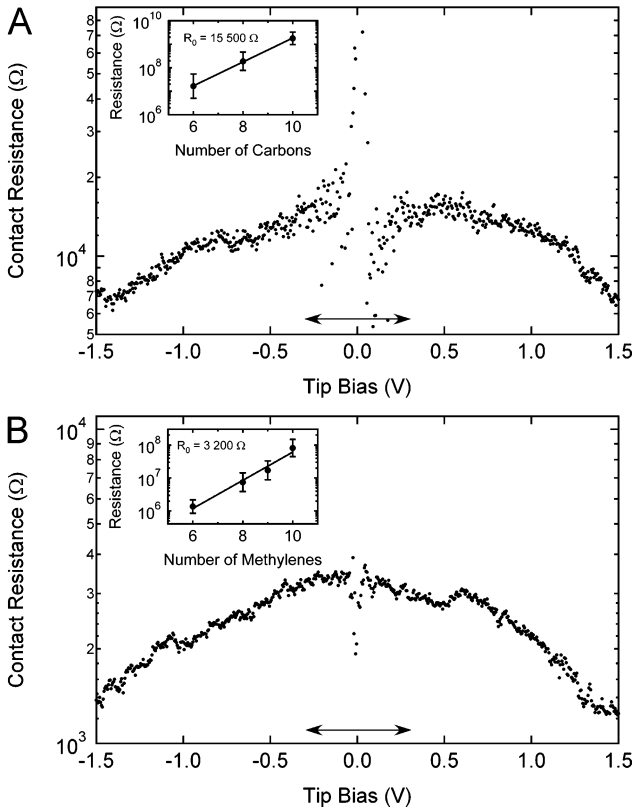

Figure 5. Contact resistance (R_0) as a function of applied bias for single representative Au−alkanethiol−Au (A) and Au−alkanedithiol−Au (B) junctions. Insets show the contact resistance calculated near zero bias as determined by fitting the linear behavior between ±0.3 V (see arrow). Scatter near zero bias in the primary graphs is due to error in fitting the data on a point-by-point basis. Decrease in R_0 is analogous to the decrease observed in Figure 4.

zero bias in Figure 5. This is an artifact of the extrapolation and should be disregarded. In this low-bias regime, currents are linear and R_0 can be determined more accurately by the method used in Figure 3. The inset graphs of Figure 5 show the calculated low bias R_0 values for the specific junctions displayed in the primary graphs. The values of R_0 obtained in the insets correspond well with the apparent crest in the related R_0 versus V plot.

Work Function and Bias Dependence of the Junction Tunneling Efficiency (β). Length dependent measurements are useful to describe how efficiently electrons can tunnel through molecular bonds. More efficient tunneling is characterized by lower β values. In the previous section, we have illustrated how changes in the Fermi level due to changes in the electrode work function and applied bias affect the contact resistance in molecular junctions. In this section, we show that these same changes do not have an effect on the attenuation of current by the molecular chain. Figure 6 shows no trend in measured β values with work function for junctions composed of either alkanethiols or alkanedithiols. Further, the β values are the same for alkanethiols and alkanedithiols. For all 18 junction types, the average β value measured was 1.1 per carbon atom (C^{-1}) or 0.88 $Å^{-1}$ in agreement with most of the literature.[3,13,15,33,34] The bias dependence of β similarly shows no trend (see Figure 7). The correspondence between Figures 6 and 7 is analogous to the correspondence of R_0 with work function and applied

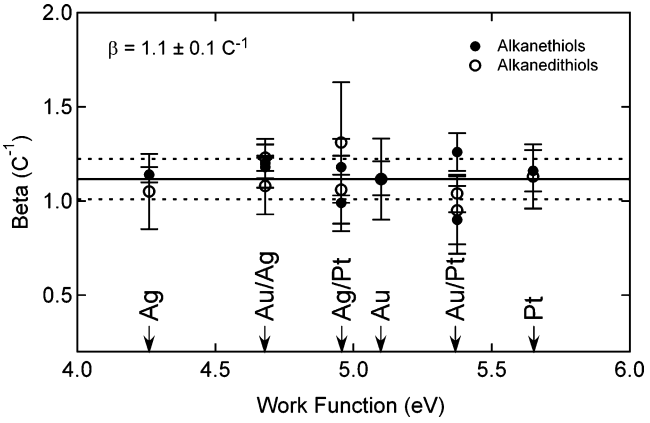

Figure 6. β as a function of electrode metal work function for junctions composed of alkanethiols (●) and alkanedithiols (○). No trend is observed, and the solid line is the average of the 18 data points (1.1 C^{-1}). Dashed lines are one standard deviation above and below the average.

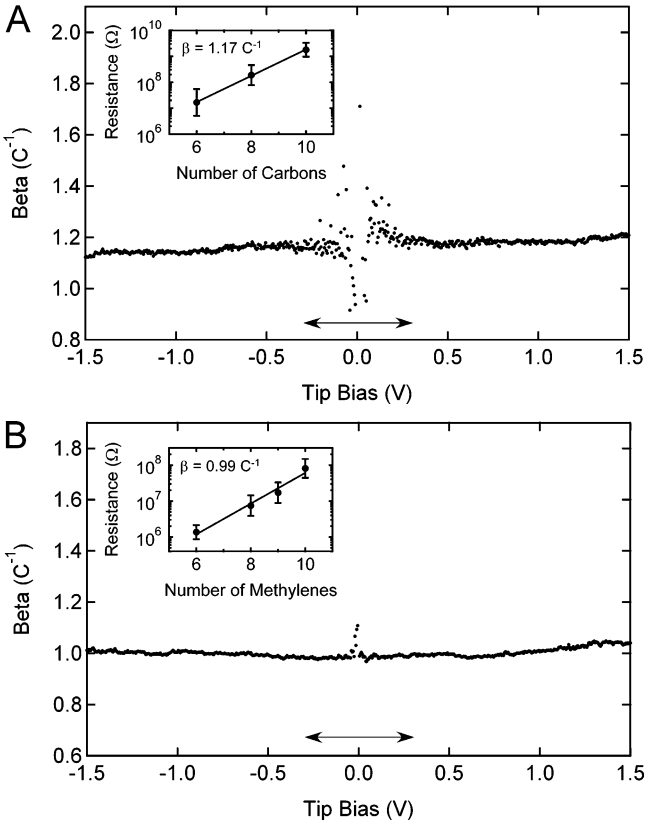

Figure 7. β as a function of applied bias for a single representative Au−alkanethiol−Au (A) and Au−alkanedithiol−Au (B) junction. Insets show β calculated near zero bias as determined by fitting the linear $I-V$ behavior between ±0.3 V (see arrow). Scatter near zero bias in the primary graphs is due to error in fitting the data on a point-by-point basis. Behavior is analogous to that seen in Figure 6.

bias as seen in Figures 4 and 5. Low bias artifacts are also present in Figure 7 due to the method of calculation. The insets show extrapolated low-bias β values that are in agreement with the trend in the respective primary graphs.

Discussion

Dependence of R_0 and β on Electrode Work Function and Applied Bias. A first attempt toward understanding the dependence of R_0 and β on the position of the Fermi level (both in terms of electrode work function and applied bias) involves

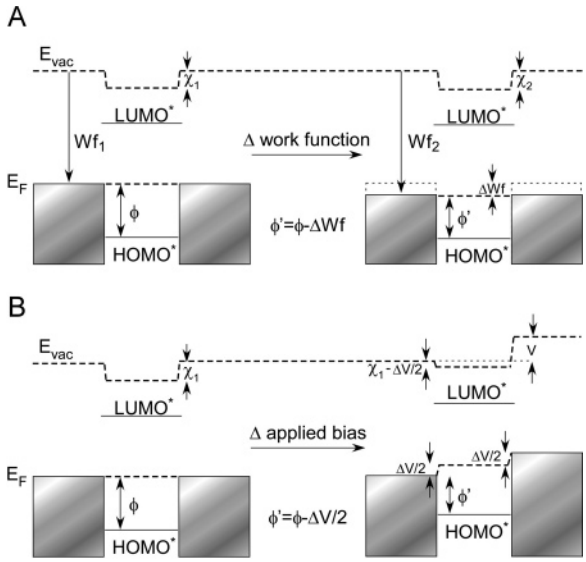

Figure 8. Changes in effective tunneling barrier ($\phi \rightarrow \phi'$) corresponding to a 1 eV change in metal work function (A) and to a 2 V applied bias with $\eta = 0.5$ (B). Contacts are assumed to be symmetric with vacuum level shifts (χ) of approximately −1.4 eV.[55]

consideration of the simple energy level diagrams in Figure 8, which are analogous to diagrams used to describe transport in conventional semiconductor and tunneling junctions. Figure 8 shows energy diagrams in which two metal electrodes are used to contact a molecule. The Fermi level of the junction is established somewhere between the HOMO* and LUMO* levels of the molecule.[46] Electrodes with higher work functions result in lower barriers (ϕ) to transport as illustrated in Figure 8A. The observed reduction of R_0 with increased electrode work function (Figure 4) is consistent with this picture and indicates that the Fermi level is closer to the HOMO* than to the LUMO*. Likewise, according to Figure 8B, application of a voltage to the junction results in a reduced barrier, consistent with the observed trend in R_0 versus bias in Figure 5. The order of magnitude correlation between Figures 4 and 5 can also be crudely explained by the barrier models of Figure 8. Roughly speaking, a change of 1 V in metal work function corresponds to a 2 V change in applied bias if one assumes a symmetric voltage drop across each contact.[47,48] Therefore, a similar reduction of the barrier occurs when either a volt of bias is applied or the electrode work function is changed by a half of an electronvolt.

The trend of decreasing R_0 with increasing work function is indicative of hole transport in these junctions, where the Fermi level is nearer the HOMO* than the LUMO*. This behavior can be understood in terms of the offset, ϕ, between the Fermi level in the junction and the molecular energy levels. As the metal work function is increased, the Fermi level becomes closer to the molecular HOMO*, thereby *decreasing* the effective barrier, ϕ, to transport through the junction. Figure 8 is simply a first-order model, and there are undoubtedly other factors that

(46) HOMO* and LUMO* refer to the HOMO and LUMO levels of the methylene chain. The true HOMO and LUMO levels are the highly localized bonding and antibonding orbitals resulting from the S−Au bond.
(47) It is generally believed that some fraction of the applied bias in a molecular tunnel junction is dropped at each contact (η and $1 - \eta$). In the case of perfectly symmetric $I-V$ characteristics $\eta = 0.5$.
(48) Datta, S.; Tian, W.; Hong, S.; Reifenberger, R.; Henderson, J. I.; Kubiak, C. P. *Phys. Rev. Lett.* **1997**, *79*, 2530−2533.

contribute to R_0 such as charge transfer at the electrode interfaces and the actual density of states in the electrodes.

The fact that there is no apparent trend in the β values with Fermi level position (varied either by metal work function or applied bias) makes it more difficult to apply the simple energy level model in Figure 8. At first glance, one expects from Figure 8 that β *should* depend on metal type. However, it is possible that although ϕ depends on metal work function, the Fermi level lies well within the large HOMO*−LUMO* gap (∼8−10 eV) for the methylene chain, such that altering ϕ by a couple of volts does not bring the junction near enough to resonance with the HOMO* to observe a decrease in β. Alternatively, it is possible that the Fermi level in the molecule is somehow pinned with respect to the HOMO* and LUMO* positions such that the final offset between the junction Fermi level and the molecular states will not be different for different metal contacts.[49] Charge transfer at the metal−molecule interfaces would then result in different barriers to transport *localized* at the contact, which would be reflected in R_0. In this second case, the β dependence on Fermi position would be essentially nonexistent, and increase in electrode work function and applied bias would tend to decrease interfacial dipoles, thereby reducing R_0.

In the framework of each of these explanations, it can be argued that increasing the electrode work function or applying bias will reduce the interfacial barrier (R_0) although transport along the molecule will be weakly affected. Each situation is an extremum, where the Fermi position is determined entirely by either the contacts or by the molecule, and it may be possible that elements of each of these hypotheses are correct. The difficulty in rationalizing the above effect indicates that details of transport in molecular junctions are not adequately addressed by simple models based essentially on a square barrier.

Inadequacies of the Simmons Model. As stated earlier, the Simmons equation predicts the general shape of $I-V$ traces in molecular junctions. The exponential length dependence of the current is also predicted according to eq 1. In the case of highly insulating oxide tunnel junctions, the approximation of a single square energy barrier equal in height to the offset between the Fermi level and the oxide valence band (the Fermi level and the vacuum level in the case of an air tunnel junction) works well.[50,51] However, there exists relatively strong electronic coupling through a tunnel junction composed of molecules. As a result, fitting molecular junction data to the three-parameter Simmons equation becomes ambiguous because the fit parameters can have physically unreal values.

For example, it is difficult for the Simmons equation to discriminate between A and s as can be seen by comparing the values in the inset tables of Figure 2. The value of s in eq 1 should increase with molecular length; however, the fit does not predict this. Instead, there is a general decrease in A and a slight increase in the barrier ϕ. A given Simmons fit only involves one chain length, so it is not surprising that the exponential decrease of the current (observed as an effect of increasing molecular length) may be accounted for in the model by either a decreasing junction area or an increasing barrier length. If the fits are done by forcing the length parameter to increase as expected, the predicted areas increase dramatically in order to compensate for the increased length, and the barrier increases to as large as 7 eV. The fit cannot predict the amount of measured current for the longer chain molecules without the area increasing to physically unreasonable values ($>10^{16}$ nm^2). The relationship between A and ϕ is complicated in this analysis. A increases both to compensate for the increasing s and the increasing ϕ. However, ϕ must increase to describe the shape of the $I-V$ curve and, if interpreted as the position of the HOMO* relative to the Fermi level, cannot be smaller than 3 eV because no conductance peaks are observed out to 1.5 V ($\phi/2$).

There also exists an inconsistency in the model involving the barrier height. According to eq 4, the measured β value should be an independent measure of the barrier. The measured value of β (1.1 C^{-1} or 0.88 Å^{-1}) corresponds to a barrier of 0.73 eV, which is significantly smaller than what could be predicted from a fit of the $I-V$ data. This value also seems to be too low in light of ultraviolet photoelectron spectroscopy (UPS) experiments that show the molecular HOMO* position to be about 5 eV from the Fermi level in octadecanethiol monolayers on Au.[52−55] This problem probably arises because of the simplistic model from which the Simmons equation is derived: that of a single energy barrier with height ϕ between two metal electrodes. Such a barrier does not adequately describe the situation for a molecule chemically bound between two electrodes. Instead of a single energy level, a density of states arises in the molecular junction as a result of the mixing of molecular orbitals and metal electrodes.[56−58] Therefore, the interpretation of ϕ in eqs 1 and 4 cannot be as simple as an offset of the Fermi level and the energy of a molecular state, but rather it can be thought of as an effective barrier to transport. The effective barrier is smaller than would be predicted due to the in-gap DOS that results from coupling of the molecule to the electrodes. The broadening of the molecular states has the effect of improving the electronic transmission. Instead of being described by a single tunnel barrier of ∼5 eV, the effective barrier must be described as an integration over many barriers according to the DOS, thereby reducing the effective barrier to ∼1 eV as determined from the measured β value.

Transmission Theory. Correct modeling of the resistance of molecular junctions involves careful quantum mechanical consideration of the orbital overlaps between one electrode and the molecule, through the bridge sites of the molecule, and

(49) Tomfohr, J. K.; Sankey, O. F. *Phys. Rev. B* **2002**, *65*, 245105/245101−245105/245112.
(50) Dorneles, L. S.; Schaefer, D. M.; Carara, M.; Schelp, L. F. *Appl. Phys. Lett.* **2003**, *82*, 2832−2834.
(51) Seine, G.; Coratger, R.; Carladous, A.; Ajustron, F.; Pechou, R.; Beauvillain, J. *Phys. Rev. B* **1999**, *60*, 11045−11050.
(52) Duwez, A. S.; Di Paolo, S.; Ghijsen, J.; Riga, J.; Deleuze, M.; Delhalle, J. *J. Phys. Chem. B* **1997**, *101*, 884−890.
(53) Whelan, C. M.; Barnes, C. J.; Walker, C. G. H.; Brown, N. M. D. *Surf. Sci.* **1999**, *425*, 195−211.
(54) Kera, S.; Setoyama, H.; Kimura, K.; Iwasaki, A.; Okudaira, K. K.; Harada, Y.; Ueno, N. *Surf. Sci.* **2001**, *482−485*, 1192−1198.
(55) Alloway, D. M.; Hofmann, M.; Smith, D. L.; Gruhn, N. E.; Graham, A. L.; Colorado, R., Jr.; Wysocki, V. H.; Lee, T. R.; Lee, P. A.; Armstrong, N. R. *J. Phys. Chem. B* **2003**, *107*, 11690−11699.
(56) Tian, W.; Datta, S.; Hong, S.; Reifenberger, R.; Henderson, J. I.; Kubiak, C. P. *J. Chem. Phys.* **1998**, *109*, 2874−2882.
(57) Datta, S. *Superlattices Microstruct.* **2000**, *28*, 253−278.
(58) Xue, Y.; Datta, S.; Ratner, M. A. *J. Chem. Phys.* **2001**, *115*, 4292−4299.

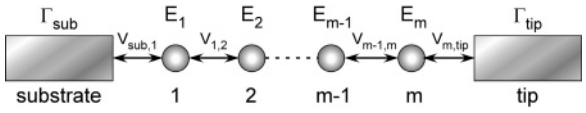

Figure 9. Schematic representation of a molecular bridge composed of *m* sites sandwiched between two electrodes labeled substrate and tip. Each site has a corresponding energy (E_i) and an overlap energy with its neighboring site ($V_{i,i+1}$). The effects of the semi-infinite electrodes are expressed in terms of the energy terms Γ_{sub} and Γ_{tip}.

between the molecule and the other electrode. The resistance (R) of the junction is described by the Landauer equation:[59]

$$R = \frac{h}{2e^2NT} \tag{5}$$

where N is the number of molecules in the junction (assuming that the molecules can be thought of as resistors in parallel and that cooperative effects are weak and that the molecules in the junction are contacted equally well), and the transmission function (T) is determined by the net orbital overlap between electrodes. The prefactor $2e^2/h$ is the quantum unit of conductance and has the value of 77.3 μS. Figure 9 shows a scheme of a molecular junction with m bridge sites with site energy E_i and overlap energies $V_{i,i+1}$. The effect of the infinite electrodes is encompassed in the Γ_{sub} and Γ_{tip} terms. The transmission of the junction can be determined (in the weak coupling limit) by combining these energies as follows:[60]

$$T(E_F) = 16 \cdot \frac{|V_{sub,1} \cdot V_{m,tip}|^2}{\Gamma_{sub}(E_F) \cdot \Gamma_{tip}(E_F)} \cdot \left|\prod_{i=1}^{m-1} \frac{V_{i,i+1}}{E_i - E_F}\right|^2 \cdot \frac{1}{(E_m - E_F)^2} \tag{6}$$

In the experiments reported here, the chain is either an alkanethiol molecule or an alkanedithiol molecule, such that the first site in the chain is a sulfur atom and the m-th site is either a methyl group or a sulfur atom, respectively. The rest of the chain consists of n methylene sites that we will consider to be identical. This leads to the following equations for the junction transmission:

$$T(E_F) = 16 \cdot \frac{|V_{sub,S} \cdot V_{CH_3,tip}|^2}{\Gamma_{sub}(E_F) \cdot \Gamma_{tip}(E_F)} \cdot \frac{|V_{S,C}|^2}{(E_S - E_F)^2} \cdot \frac{|V_{C,C}|^{2(n-1)}}{(E_C - E_F)^{2n}} \quad \text{-alkanethiol junctions} \tag{7a}$$

$$T(E_F) = 16 \cdot \frac{|V_{sub,S} \cdot V_{S,tip}|^2}{\Gamma_{sub}(E_F) \cdot \Gamma_{tip}(E_F)} \cdot \frac{|V_{S,C}|^4}{(E_S - E_F)^4} \cdot \frac{|V_{C,C}|^{2(n-1)}}{(E_C - E_F)^{2n}} \quad \text{-alkanedithiol junctions} \tag{7b}$$

Equations 7a,b can be written such that they are divided into three factors: one that involves the substrate contact (T_{sub}), the tip contact (T_{tip}), and the molecule (T_{mol}):

$$T(E_F) = T_{sub} \cdot T_{tip} \cdot T_{mol} \tag{8}$$

where

$$T_{sub} \equiv \frac{4}{\Gamma_{sub}(E_F) \cdot V_{C,C}} \cdot \left|\frac{V_{sub,S} \cdot V_{S,C}}{E_S - E_F}\right|^2 \tag{9a}$$

$$T_{tip} \equiv \frac{4 \cdot |V_{CH_3,tip}|^2}{\Gamma_{tip}(E_F) \cdot V_{C,C}} \quad \text{-alkanethiol junctions} \tag{9b.1}$$

$$T_{tip} \equiv \frac{4}{\Gamma_{tip}(E_F) \cdot V_{C,C}} \left|\frac{V_{S,tip} \cdot V_{S,C}}{E_S - E_F}\right|^2 \text{-alkanedithiol junctions} \tag{9b.2}$$

$$T_{mol} \equiv \left|\frac{V_{C,C}}{E_C - E_F}\right|^{2n} = (T_{C-C})^n \tag{9c}$$

where T_{C-C} is the transmission per carbon bond. To maintain unitless T values, T_{sub} and T_{tip} must incorporate a factor of V_{C-C} and are therefore not entirely independent of the molecular structure. Substitution of eqs 8 and 9 into eq 5 shows that the resistance indeed depends exponentially on the junction length and can be modeled with eq 3. R_0 and β can be expressed in terms of eqs 9a−c as follows:

$$R_0 \equiv \frac{h}{2e^2N} \frac{1}{T_{sub}} \frac{1}{T_{tip}} \tag{10a}$$

$$\exp(\beta n) \equiv \frac{1}{T_{mol}} = \left(\frac{1}{T_{C-C}}\right)^n \tag{10b}$$

such that

$$\beta = 2 \ln\left(\frac{E_C - E_F}{V_{C,C}}\right) \tag{10c}$$

Determination of T_{sub}, T_{tip}, and T_{C-C}. The data in Figures 4 and 6 were used to provide estimates for the transmission associated with each contact (T_{sub} and T_{tip}) and molecule (T_{C-C}) studied. Equation 5 can be expressed in terms of eqs 10a,b to express the junction resistance as a function of these transmissions:

$$R = \frac{h}{2e^2N} \cdot \frac{1}{T_{sub}} \cdot \frac{1}{T_{tip}} \cdot \left(\frac{1}{T_{C-C}}\right)^n \tag{11}$$

T_{C-C} was determined by the measured β values as indicated by eq 10b. Furthermore, because it has been shown that β is independent of the junction contacts studied, T_{C-C} has one value (~0.33) for these junctions. Equation 10c predicts that this value should depend on the junction Fermi position and therefore the electrode work function and applied bias. The fact that this is not observed indicates that the percent change in ($E_C - E_F$) is not large in our experiments.

T_{sub} and T_{tip} were determined from the contact resistance data in which n is equal to zero. For each of the measured R_0 values in this report, there is a combination of one substrate transmission (T_{Pt-S-C}, T_{Au-S-C}, T_{Ag-S-C}) and one tip transmission (T_{Pt/CH_3}, T_{Au/CH_3}, T_{Ag/CH_3}, T_{Pt-S-C}, T_{Au-S-C}, T_{Ag-S-C}). As stated earlier, the reverse cases of mixed metal alkanedithiol junctions (e.g., Au−S−$(CH_2)_n$−S−Ag and Ag−S−$(CH_2)_n$−S−Au) appear to have similar resistances. Therefore, in this analysis it was assumed that the tip-sulfur and substrate-sulfur transmissions are the same for a given metal and that there were only six transmission values that needed to be solved. The 18

(59) Landauer, R. *Phys. Lett. A* **1981**, *85*, 91−93.
(60) Nitzan, A. *Annu. Rev. Phys. Chem.* **2001**, *52*, 681−750.

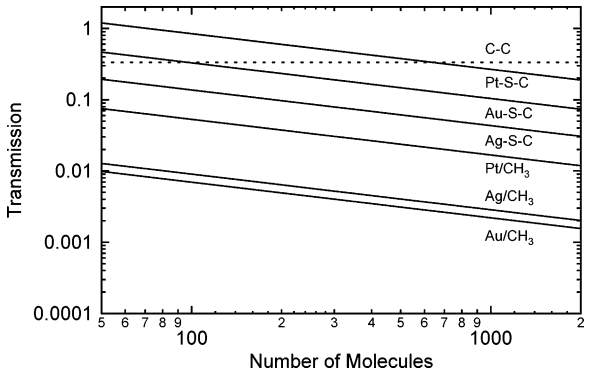

Figure 10. Contact transmissions (solid lines) interpolated from the data in Figure 4 as a function of the number of molecules present in our CP-AFM experiment. Minimization of variance was not possible in terms of the number of molecules. Therefore it remains a variable in our calculations. Choosing an estimate for the number of molecules present in our junctions allows for prediction of the transmission for each of the six different contacts. The dashed line represents the transmission of a single methylene unit (~0.33) as determined from the measured β value.

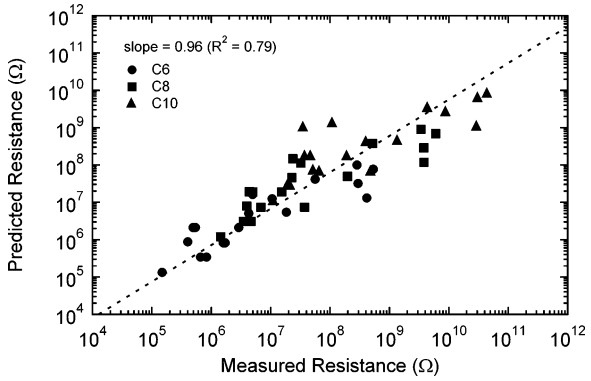

Figure 11. Log−log plot of the junction resistance as determined from the transmission values in Figure 10 for chains of 6 (C_6), 8 (C_8), and 10 (C_{10}) methylene units versus the average measured junction resistance for the 18 metal−molecule−metal combinations studied (total of 54 points). Dashed line represents a linear least-squares fit forced through zero. The slope of 0.96 (near unity) indicates that the transmission model fits the data correctly.

measured contact resistances over-specified these six T values so that a minimization of variance was performed. To do this, eq 11 was linearized and a relative residual value (ϵ) was defined for each of the 18 experiments:

$$\epsilon = \frac{\ln\left(\frac{2e^2NR_0}{h}\right) - \ln\left(\frac{1}{T_{sub}}\right) - \ln\left(\frac{1}{T_{tip}}\right)}{\ln\left(\frac{2e^2R_0}{h}\right)} \qquad (12)$$

The sum of the squared residual values was used to define a variance (V) as a function of the six T values and N:

$$V = \sum_{i=1}^{18}(\epsilon_i)^2 \qquad (13)$$

The error in the system of equations was minimized by setting the partial derivatives of V with respect to each ln(1/T) term ($T = T_{Pt/CH_3}$, T_{Au/CH_3}, T_{Ag/CH_3}, T_{Pt-S-C}, T_{Au-S-C}, and T_{Ag-S-C}) equal to zero, which provided T values that were functions of the number of molecules (N) present in our experiment (see Figure 10). V could not be simultaneously minimized with respect to N because it simply acts as a scaling factor. Therefore, values for each T were determined as a function of *assumed* values for N as shown in Figure 10. In other words, the parameters that were determined by minimization of variance were the products of N and the various T values. Values of T can only be acquired if one first assumes a value for N. The exact number of molecules in our experiment is not unambiguously known; however, using contact mechanics (i.e., the Derjaguin−Muller−Toporov model), we believe it ranges between 100 and 1000. We also assume that this value is constant for each of the 18 metal−molecule−metal combinations because of the similarity in tip radii and the data averaging. It is also important to note that the values of T_{sub} and T_{tip} are not completely independent of the molecular structure (they include a V_{C-C} factor) and are therefore only applicable to saturated alkane systems.

Figure 10 shows that the predicted contact transmission values are significantly lower for physisorbed contacts versus chemisorbed ones. In terms of eqs 9a,b this is likely due to the ineffective coupling of the electrode and the methyl terminus of the molecule ($V_{CH_3,tip}$) as compared to the covalently bonded chemisorbed contact ($V_{S,tip}$).[5,10,22,31] Higher work function chemisorbed contacts also result in higher transmissions as observed in the ranking: $T_{Pt-S} > T_{Au-S} > T_{Ag-S}$. This is not necessarily the case for physisorbed contacts as T_{Ag/CH_3} appears to be slightly larger than T_{Au/CH_3}. Seminario et al. predict a similar ranking of transmission values for the chemisorbed contacts.[29] However, these predictions involve a benzene ring with two chemisorbed contacts so that comparison of actual values may not be appropriate. The work function and bias dependence of R_0 can be expected considering eqs 9a,b. Γ_{sub} and Γ_{tip} are functions of the Fermi level, and the overlap energies between the metal and the molecule ($V_{sub,S}$, $V_{S,tip}$, $V_{CH_3,tip}$) are likely to depend on the metal and the applied bias. Effects caused by interface dipoles would also be observed in these quantities.

Using the values in Figure 10, junction resistance values were generated for the 18 contact combinations, each incorporating a C_6, C_8, or C_{10} molecule. In Figure 11, these calculated values are plotted against the measured values to demonstrate the goodness of fit for eqs 12 and 13. A slope of 0.96 (1.0 is ideal) is found when a least-squares regression is done on the log−log axis with the intercept forced through zero. This confirms that our calculations of T for the different contact types are all self-consistent. The spread in the data points of Figure 11 is indicative of the variance associated with our measurements. This paper offers a novel attempt to extract values of electronic transmission for the contacts and molecular backbone separately based on experimental resistance measurements. Future experiments that measure junction resistances with higher precision will offer better agreement between predicted resistances and measured resistances.

Conclusions

Molecular tunnel junctions were formed using CP-AFM to contact SAMs on polycrystalline metal films. Effects of contact work function and applied bias were studied in 18 different junction types incorporating all variations of the three metals (Pt, Au, or Ag) on the substrate and tip, with alkanethiol or alkanedithiol bridging molecules. Length-dependent measurements were made to extract values for the structure-dependent attenuation factor, β, as well as the contact resistance (R_0).

R_0 was found to decrease with increasing electrode work function and increased applied bias. Junctions composed of different tip and substrate metals displayed contact resistances between those of junctions composed only of either metal. The decrease in resistance can be attributed to a decrease in the barrier height between the metal Fermi level and the molecular HOMO* or a smaller interface dipole that results from Fermi level alignment with higher work function metals. In terms of the Landauer equation, values of contact transmission can be extracted from the measurements of contact resistance. We demonstrated that chemisorbed contacts have a much higher transmission than physisorbed contacts and that the transmission of the chemisorbed contact is larger when the work function is larger. We also showed that the resistance of doubly bound alkanedithiol molecules is about 1 to 2 orders of magnitude lower than singly bound alkanethiol molecules. Unlike R_0, the β value exhibited no trend with electrode work function or applied bias in these junctions. Furthermore, no difference in β was found between junctions composed of alkanethiols and alkanedithiols. It is likely that the Fermi level in these junctions is well within the HOMO*−LUMO* gap of the molecules and therefore changes in the Fermi level of a couple of eV are not adequate to see an improvement in tunneling efficiency as the transport remains dominated by the low DOS in the gap.

Acknowledgment. C.D.F. thanks the NSF (DMR-0084404, CHE-0315165) for financial support.

JA046274U